

Interaction Mechanics between Embedded Micro-Actuators and the Surrounding Host in Smart Structures

A. DASGUPTA AND A. ALGHAMDI

ABSTRACT

The mechanical interactions between "smart" host structures and embedded distributions of piezoelectric microsensors and microactuators are analyzed using Eshelby's classical equivalent inclusion technique. A first order estimate of the changes in the mechanical energy of the system due to actuation loads is obtained through appropriate simplifying assumptions. Preliminary linearized results are presented for PZT-5H devices embedded in a simply supported ALPLEX isotropic beam. Results are also presented for strain concentrations in the host around the embedded microdevice, as a result of external and actuation loads.

These results of the interaction mechanics provide preliminary insights for (i) obtaining accurate transfer functions for control of the structure; and (ii) assessing the damage (and associated loss of reliability) caused to the host and to the actuator by external environmental loads as well as internal actuation loads.

INTRODUCTION

The concept of "smart" or adaptive materials/structures involves host structures with either embedded or surface-mounted sensors, actuators and associated electronic hardware, which provide the structure with the capability to sense external stimuli and to adaptively respond to them. For example, distributed networks of sensors and actuators may be used for sensing and actively damping vibrations in large flexible space structures through the use of closed-loop control algorithms. Commonly used "active" materials for combined sensing/actuation capabilities include piezoelectric, electrostrictive, magnetostrictive, magneto-relaxor, and shape-memory alloy materials. Fiber-optic devices can function as sensors, but not as actuators. Conversely, electro-rheological materials are primarily useful for actuation functions, rather than sensing functions. Detailed discussion of examples and capabilities of these materials is beyond the scope of this paper. Instead, the focus is on the mechanics of their interactions with the host, in particular, interactions of embedded devices with the surrounding host.

The embedded instrumentation and sensor/actuator devices act like

¹ A. Dasgupta is an Assistant Professor and A. Alghamdi is a Graduate Student in the Mechanical Engg. Dept., Univ. of Maryland, College Park, MD 20742

heterogeneities within the host structure, and inevitably perturb the local values of the field variables being sensed/controlled. The magnitude of this perturbation is a measure of the obtrusivity of the embedded device. Another consequence of the device obtrusivity is the possibility of nucleating damage in the device, or in the host, or at the interface, due to stress concentrations under external structural loads and/or under internal actuation loads. Effective control and reliability assessment of adaptive structures is therefore facilitated if explicit relationships can be developed to account for the mechanical interactions between the host and the embedded sensor/actuator inclusions.

The problem of quantifying the interactions essentially involves solving coupled electro-mechanical, magneto-mechanical, opto-mechanical or thermo-mechanical boundary value problems in heterogeneous domains, depending on the type of sensor and actuator device utilized. There have been numerous studies in the literature for modeling the interactions between sensor/actuator devices and host structures in adaptive structures of special geometries. For example, laminated assemblies of piezo-electric wafers/films in composite plates/beams have been analyzed by simple beam models [1], classical laminated plate theories [2], and small-deformation as well as large-deformation one-dimensional eigen-function approximations [3,4]. Embedded cylindrical devices such as fiber-optic sensors have been analyzed using displacement [5] and stress-function [6] formulations. Finite element formulations have also been developed for solving the coupled boundary value problems in adaptive structures with complex geometries [7-9].

This paper illustrates the role of closed-form eigenstrain methods based on Eshelby's equivalent inclusion eigenstrain techniques [10], for quantifying the mechanical interactions in a sample Euler-Bernoulli beam with embedded distributions of piezoelectrical sensor/actuator micro-devices. In the present context, the term "micro-device" implies that the size of the embedded device is at least an order of magnitude smaller than the size of the host structure and the spacing between neighboring devices. The influence of these actuators on the internal energy of the adaptive beam is investigated analytically. The internal energy term is important when investigating the dynamic characteristics of the beam. Finally, expressions are developed for the strain concentrations in the host, due to the presence of the embedded sensor/actuator micro-devices. This information is crucial for assessing the impact of the embedded devices on the reliability of the host structure.

PROBLEM STATEMENT

The application of the eigenstrain solution technique to "smart" structures is illustrated in this paper through the simple example of a simply supported slender beam. As shown schematically in Figure 1, two rows of uniformly spaced micro-devices are embedded in the beam, symmetrically about the neutral plane of the beam. Each row of devices is excited alternately, in order to control the vibrational characteristics of the beam. As the beam flexes upwards, the devices in the upper row act as sensors and their outputs are used in a closed-loop feedback circuit to actuate the lower row of devices. The actuation strain is assumed to be positive in sign. During the next half cycle, when the beam flexes downwards, the roles of the two rows of devices are reversed. The influence of the devices on the vibrational characteristics is investigated analytically by modeling the mechanical interactions between each device and the host. The aim is to generate the electro-mechanical interaction information, necessary for combining the

device response with that of the host beam, in an integrated dynamical equation of the adaptive structure.

Several simplifying assumptions are made in this approximate analytical study. Euler-Bernoulli beam theory is assumed to apply. Each embedded micro-device is assumed to be a piezoelectric cylinder of elliptical cross-section, whose polarization axis is oriented along the length of the beam. The length scale of each device is limited to at least an order of magnitude less than the beam. Hence, the bending strain is assumed to be approximately uniform over the length scale of the device. This approximation greatly simplifies the eigenstrain solution and is used in this paper for illustrative purposes only. A more rigorous analysis will be required for more accurate results, and is deferred to a future paper. Further, each device is assumed to be embedded far enough below the free surface of the beam such that Eshelby's eigenstrain solution for infinite spaces is applicable. Finally, the distance between neighboring devices is assumed to be large enough to prevent mutual interactions. Thus, this solution is only valid for dilute distributions of micro-devices.

As a result of the assumptions presented above, the micro-devices are approximated to act like elastic heterogeneities embedded in an infinite-dimensional host structure. Perfect bonding is assumed at the interfaces. The sensor/actuator material is assumed to be PZT-5H, and the host material is assumed to be ALPLEX plastic. All materials are approximated to be linear and mechanically isotropic. The linearizing assumption limits the validity of this approximate analysis to small excitation voltages and small deformations. The assumption of mechanical isotropy is an acceptable approximation for most PZT materials.

ANALYSIS

Eshelby's classical equivalent-inclusion technique [10] is applied to obtain the elastic interaction fields, both in the device and in the host, under external applied loads and under internal actuation loads. External loads are handled through Eshelby's fictitious eigenstrain technique. Internal actuation loads are treated as a real eigenstrains and are obtained from the linearized, isothermal, coupled electro-mechanical constitutive models given below. The difference between PZT sensors and actuators in the present analytical context is that the sensor only has a fictitious eigenstrain due to external loads, while the actuator has both fictitious and real eigenstrains.

The linearized, isothermal, coupled electro-mechanical constitutive model is [11]:

$$\begin{aligned}\bar{\sigma} &= \underline{S} \bar{\epsilon} - \bar{h}^T \bar{E} \\ \bar{D} &= \underline{h} \bar{\epsilon} + \underline{\epsilon} \bar{E}\end{aligned}\quad (1)$$

where $\bar{\epsilon}$ is the total strain vector including mechanical as well as electro-mechanical contributions, $\bar{\sigma}$ is the mechanical stress vector, \bar{E} is the electrical field vector, \bar{D} is the electrical displacement vector. \underline{S} is the mechanical compliance tensor (assumed

to be isotropic in this approximate analysis), \underline{h}^T is the piezoelectric coupling tensor indicating the stress caused by completely constrained excitation of the PZT material under a unit applied electrical field, $\underline{\epsilon}$ is the dielectric tensor for the PZT material. Arrows over a quantity are used to denote vector quantities, while an underscore is used to denote tensor quantities. Clearly, only the mechanical portion of this constitutive model applies to the ALPLEX host material.

Eshelby's method [10] is based upon postulating an equivalent inclusion with a fictitious eigenstrain which has the same stress field as the real heterogeneity, under both external loads and internal actuation strains. Thus, in the heterogeneity:

$$\begin{aligned}\bar{\sigma}^o + \bar{\sigma}' &= \underline{C}^D (\bar{\epsilon}^o + \bar{\epsilon}' - \bar{\epsilon}^r) \\ &= \underline{C}^H (\bar{\epsilon}^o + \bar{\epsilon}' - \bar{\epsilon}^*)\end{aligned}\quad (2)$$

$$\text{where } \bar{\epsilon}^* = \bar{\epsilon}^r + \bar{\epsilon}^f$$

\underline{C} is the material stiffness tensor; superscripts D and H on the stiffness indicate the PZT device and the ALPLEX host, respectively; superscripts o, ', r, f and * on the stress and strain terms indicate applied far-field value, perturbation due to the presence of the heterogeneity, real actuation eigenstrains, fictitious eigenstrains due to external loading, and total eigenstrains, respectively.

The real actuation eigenstrain is obtained from Equation (1) as:

$$\begin{aligned}\bar{\epsilon}^r &= \underline{d}^T \bar{E} \\ \text{where } \underline{d}^T &= \underline{S} \underline{h}^T\end{aligned}\quad (3)$$

\underline{d}^T represents the free-expansion of the piezoelectric actuator for a unit applied electric field.

The total eigenstrain is now related to the disturbance strain by Eshelby's strain concentration tensor \underline{S}^E :

$$\bar{\epsilon}' = \underline{S}^E \bar{\epsilon}^* = \underline{S}^E (\bar{\epsilon}^r + \bar{\epsilon}^f) \quad (4)$$

Eshelby's strain concentration tensor can be computed for infinite spaces by using Kelvin's fundamental three-dimensional elasticity result for point loads [12]; and for half-spaces by using appropriate Green's functions [12]. Explicit forms for Eshelby's tensor are readily available in the literature for embedded isotropic heterogeneities of ellipsoidal geometries. Solutions for anisotropic cases may be obtained numerically [12].

Substituting Equation (4) in Equation (2), we obtain:

$$\underline{C}^D (\bar{\epsilon}^o + \underline{S}^E \bar{\epsilon}^* - \bar{\epsilon}^r) = \underline{C}^H (\bar{\epsilon}^o + \underline{S}^E \bar{\epsilon}^* - \bar{\epsilon}^f - \bar{\epsilon}^r) \quad (5)$$

Equation (5) can now be solved for the unknown fictitious eigenstrain $\bar{\epsilon}^f$ in terms of the applied external bending strain $\bar{\epsilon}^0$ and the real actuation eigenstrain $\bar{\epsilon}^r$. This completes the solution for the total stress and strain fields within the micro-device, which can now be determined from Equation (2). If the applied strain is uniform, so is the fictitious eigenstrain. Nonuniform applied strains can be approximated by a polynomial series which yields a series solution for the fictitious eigenstrain [12]. In the present problem, the far-field applied strain is assumed, as a first order approximation, to be uniform over the length scale of each embedded micro-device, in view of the simplifying assumptions stated in the previous section.

The stress and strain fields outside the device, in the surrounding host structure are more difficult to determine by Eshelby's technique. Fortunately, the exterior field is not required when computing the mechanical energy of the system, due to the actuation. The mechanical energy contributes to the internal energy of the system, and needs to be computed when using an energy-based approach for analysing the system dynamics. For instance, under an imposed displacement field, the internal energy of the system can be written in terms of the mechanical and electrical energies as:

$$U = \frac{1}{2} \int_V \bar{\sigma}^T \bar{\epsilon} dV + \frac{1}{2} \int_V \bar{E}^T \bar{D} dV \quad (6)$$

Substituting Equation (1) in Equation (6):

$$\begin{aligned} U &= \frac{1}{2} \int_V \bar{\epsilon}^T \underline{C} \bar{\epsilon} dV + \frac{1}{2} \int_V \bar{E}^T \underline{\epsilon} \bar{E} dV \\ &= U_{mech} + U_{electr} \end{aligned} \quad (7)$$

The mechanical energy term is the focus of our interest in this paper, and results from (i) the uniform flexural field of the beam, (ii) the passive perturbation of the bending field due to the presence of the micro-devices, and (iii) the actuation field of the active micro-devices. After some manipulations (which are omitted here for brevity):

$$U_{mech} = \frac{1}{2} \int_V \bar{\epsilon}^{0T} \underline{C}^H \bar{\epsilon}^0 dV + \frac{1}{2} \int_{\Omega} \bar{\epsilon}^{*T} \underline{C}^H \underline{S}^B \bar{\epsilon}^* dV \quad (8)$$

The first term in Equation (8) is evaluated by integrating the uniform bending strain energy density throughout the domain V of the beam. The second term represents energy due to the imaginary and real eigenstrains, and requires evaluation only over the domain Ω of the microdevices. Hence, the exterior solutions for the real and fictitious eigenstrain problems are not required in this study. Equation (8) is expanded further for clarity, as follows:

$$\begin{aligned} 2U_{mech} &= \int_V \bar{\epsilon}^{0T} \underline{C}^H \bar{\epsilon}_0 dV + \int_{\Omega} \bar{\epsilon}^{fT} \underline{C}^H \underline{S}^B \bar{\epsilon}^f dV + \\ &\int_{\Omega} \bar{\epsilon}^{rT} \underline{C}^H \underline{S}^B \bar{\epsilon}^r dV + \int_{\Omega} \bar{\epsilon}^{fT} \underline{C}^H \underline{S}^B \bar{\epsilon}^r dV + \int_{\Omega} \bar{\epsilon}^{rT} \underline{C}^H \underline{S}^B \bar{\epsilon}^f dV \end{aligned} \quad (9)$$

The first term in Equation (9) represents the energy of the homogeneous applied bending field. The second term is the only one dependant on the fictitious eigenstrain, which is a function of the applied bending field. The last three terms are the only ones dependent on the applied actuation eigenstrain.

In order to perform the integrations in Equation (9), all that remains now is to assume explicit representations for the applied flexural strain field, and the actuation eigenstrain. For example, in the Rayleigh scheme for estimating the natural frequency of conservative systems, an approximate displacement field can be assumed. In this example, the approximate bending field is assumed to be harmonic in time and sinusoidal in space:

$$w = \sum_n a_n \sin \omega_n t \sin \frac{n\pi y}{L} \quad (10)$$

where the y axis is oriented along the length of the beam, w is the transverse displacement in the z direction, ω_n and a_n are the natural frequency and amplitude, respectively, of the n^{th} mode, L is the length of the beam, and t is time. Only the fundamental mode ($n=1$) is of interest in this study. Thus the only non-zero term in the

bending strain field ϵ^0 is ϵ_2^0 , and is given as:

$$\epsilon_2^0 = z \frac{\pi^2}{L^2} a_1 \sin \omega_1 t \sin \frac{\pi y}{L} \quad (11)$$

where, z is the distance of the microdevice from the neutral axis of the beam. The only non-zero component of the actuation voltage vector is now E_2 . This term is now assumed to be proportional to the output of the sensory devices, and hence, to the bending deformations. Thus E_2 is written as:

$$E_2 = E_2^* \sin \omega_1 t \sin \frac{\pi y}{L} \quad (12)$$

where the amplitude E_2^* is assumed to be proportional to the amplitude a_1 of the fundamental vibrational mode of the beam:

$$E_2^* = K a_1 \quad (13)$$

The non-zero terms of the actuation strain vector are now written as:

$$\epsilon_i^r = d_{i2} E_2 \quad , \quad i = 1-3 \quad (14)$$

Equations (10-14) are used in Equation (9) to compute the mechanical energy in the system. The maximum energy during the cycle is of particular interest, for example, either in the Rayleigh scheme for estimating the fundamental natural frequency of the

homogeneous problem, or when investigating active instability suppression in slender structural members under compressive loading. Sample results, for maximum mechanical energy in the adaptive beam structure, are presented in the next section.

Finally, the strain concentrations caused by the actuator microdevices in the device and in the host are of great interest for evaluating the reliability of the "smart" system. The strain field in the device is obtained from Equation (2). Evaluation of the strain field in the host generally requires knowledge of the exterior solution for the eigenstrain problem. However, the strain and stress concentrations in the host are usually at the interface with the device and can be evaluated by superposing the interior solution with the appropriate jump functions across the interface[10]:

$$\vec{\epsilon}_{ext} = \vec{\epsilon}_{int} + \Delta\vec{\epsilon} \quad (15)$$

where subscripts ext and int represent the solutions immediately outside and inside the interface, respectively. $\Delta\vec{\epsilon}$ indicates the strain jump function which is available in the literature for ellipsoidal heterogeneities [10]. Sample strain concentration plots for combined external bending and internal actuation loads are presented in the next section.

RESULTS AND DISCUSSIONS

The material properties assumed in this analysis for the PZT-5H sensor/actuator device and for the ALPLEX host are listed in Table 1. The piezoelectric coupling tensor d^T is obviously relevant only for the device material. The dielectric properties ϵ are not of interest in the present study.

Figure 2 shows the increase in the mechanical energy as a function of the excitation voltage for different numbers of actuators. The actuators are assumed to be evenly spaced along the y direction. For convenience, the mechanical energy is normalized with respect to that for zero electrical excitation. The voltage amplitude E_2^* is represented by the proportionality factor K (in V/m/m) of Equation (13). The increase in the mechanical energy term is a measure of the elastic stiffening of the beam due to the actuation loads. This information is important when analysing the structural dynamics and/or stability. Figure 3 illustrates the dependence of this stiffening effect on the Young's modulus of the host material. The elastic stiffness of the host material has been normalized with respect to the Young's modulus of the device material, and ranges from epoxy properties to steel properties, in this graph.

The strain concentration factors in the host as a result of the far-field bending and the actuation loads, are shown in figure 4, as a function of θ . As an example, the actuation strain is assumed to be equal to the bending strain. The strain concentration factors are obtained by normalizing the principal strain values in the host (at the interface with the device) with respect to the applied bending strain ϵ_2^0 . The maximum strain concentration is greater than 2.0, and is found to occur approximately at $\theta = 10^\circ$, for the combined load state considered. The plot will be different for different combined load states.

CONCLUSIONS

This study has presented a unified approach, based on Eshelby's technique, for addressing the interaction mechanics of microdevices embedded in an adaptive structure. This interaction information is of critical importance in active vibration and/or instability suppression applications. This technique also gives simultaneous information of the stress and strain concentrations in the host due to the obtrusivity of the sensor/actuator microdevice. Such obtrusivity information is important for designing reliable smart structures.

ACKNOWLEDGEMENTS

This research work is funded in part by a grant from the Army Research Office under their University Research Initiative. Mr. Alghamdi is a graduate student, supported by King Abdulaziz University in Jeddah, Saudi Arabia.

REFERENCES

1. Burke, S. and Hubbard, J. E., "Active Vibration Control of a Simply-Supported Beam Using a Spatially Distributed Actuator," *IEEE Control Systems Magazine*, Vol. 7, No. 6, 1987.
2. Crawley, E. F., and Lazarus, K. B., "Induced Strain Actuation of Isotropic and Anisotropic Plates," *Proc., 30th SDM Conference*, Mobile, AL, 1989.
3. Wang, B-T. and Rogers, C. A., "Modeling of Finite-Length Spatially -Distributed Induced Strain Actuators for Laminated Beams and Plates," *J. Intelligent Material Systems and Structures*, Vol. 2, 1991.
4. Im, S. and Atluri, S. N., "Effects of a Piezo-Actuator on a Finitely-Deformed Beam Subjected to General Loading," *AIAA J.*, Vol. 27, No. 12, 1989.
5. Sirkis, J. S., "A Unified Approach to Phase-Strain-Temperature Models for Smart Structure Interferometric Optical Fiber Sensors," Submitted to *Optical Engineering*, 1992.
6. Dasgupta, A., and Sirkis, J. S., "The Importance of Coatings to Optical Fiber Sensors Embedded in Smart Structures," *AIAA J.*, Vol. 30, No. 5, 1992.
7. Allik H. and Hughes, T. J., "Finite Element Method for Piezoelectric Vibration," *Intl J. Num. Meth. Engg.*, Vol. 2, 1970.
8. Tzou, H. S. and Tseng, C. I., "Distributed Piezoelectric Sensor/Actuator Design for Dynamic Measurement/Control of Distributed Parameter Systems: A Piezoelectric Finite Element Approach," *J. Sound and Vibration*, "Vol. 138, No. 1, 1990.
9. Ha, S-K., Keilers, C. and Chang, F-K., "Analysis of Laminated Composites Containing Distributed Piezoelectric Ceramics," *J. Intelligent Material Systems and Structures*, Vol. 2, 1991.
10. Eshelby, J. D., "The Determination of the Elastic Field of an Ellipsoidal Inclusion and Related Problems," *Proc. Roy. Soc.*, A241, 1957.
11. Ikeda, T., "Fundamentals of Piezoelectricity," Oxford Science Publications, Oxford, 1990.
12. Mura, T., "Micromechanics of Defects in Solids," Martinus Nijhoff Pub., Boston, 1982.

	E (GPa)	ν	d_{21} (C/N) * 1e-12	d_{22} (C/N) * 1e-12	d_{16} (C/N) * 1e-12
PZT-5H	64	0.39	-274	593	741
ALPLEX	3.5	0.35	—	—	—

Table 1. Electromechanical Properties of Device and Host Materials.

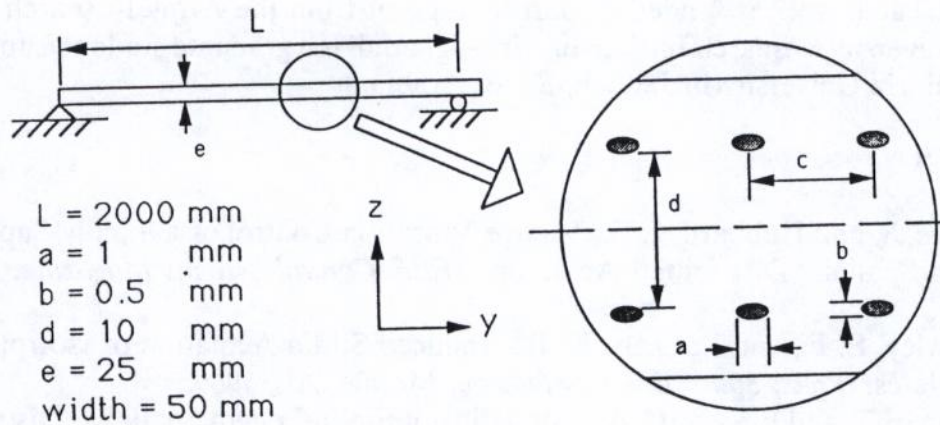


Figure 1. Schematic of Adaptive Beam with Embedded Rows of Microdevices.

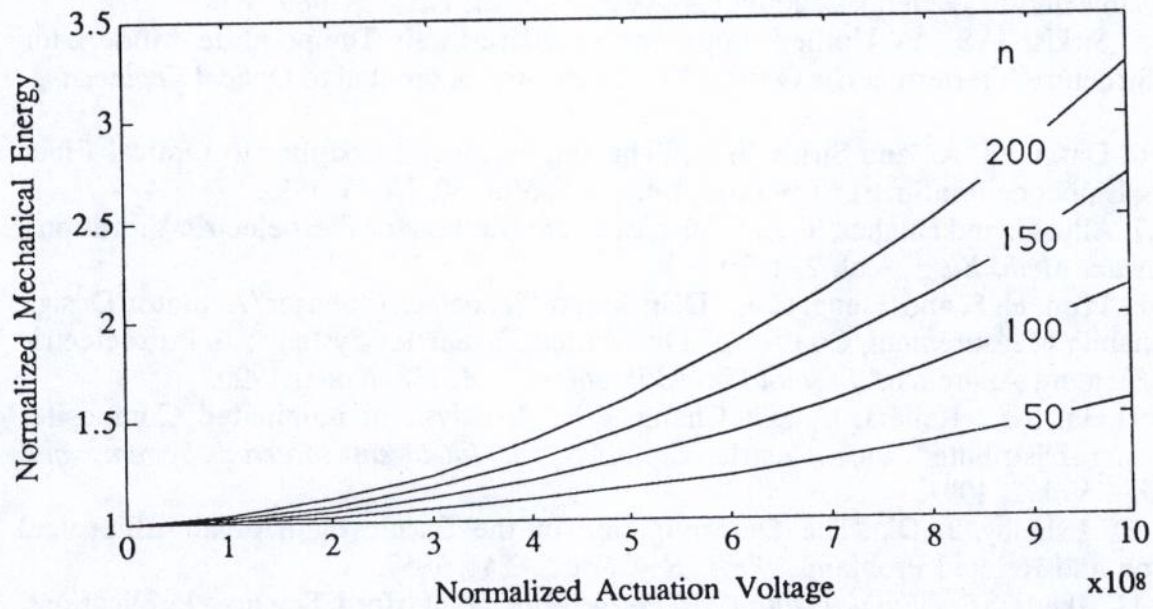


Figure 2. Normalized Mechanical Energy as a function of Normalized Excitation Voltage (V/m/m) for different device densities (n = number of active devices).

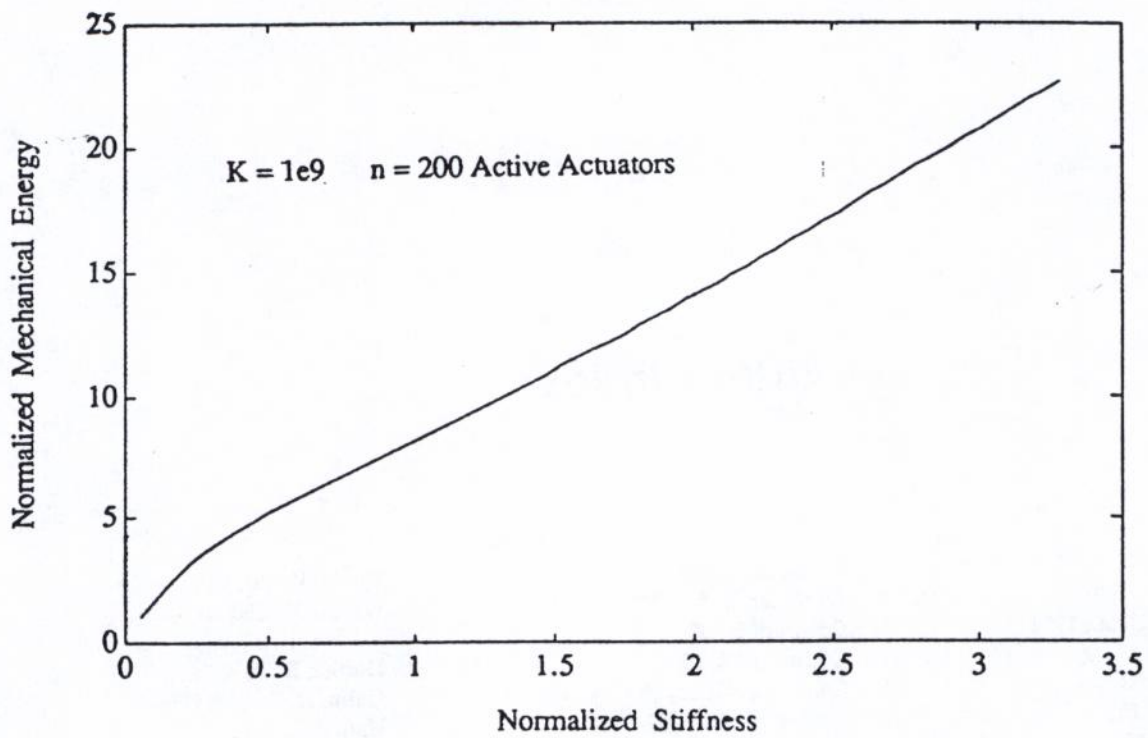


Figure 3. Plot of Normalized Mechanical Energy vs. Normalized Host Stiffness.

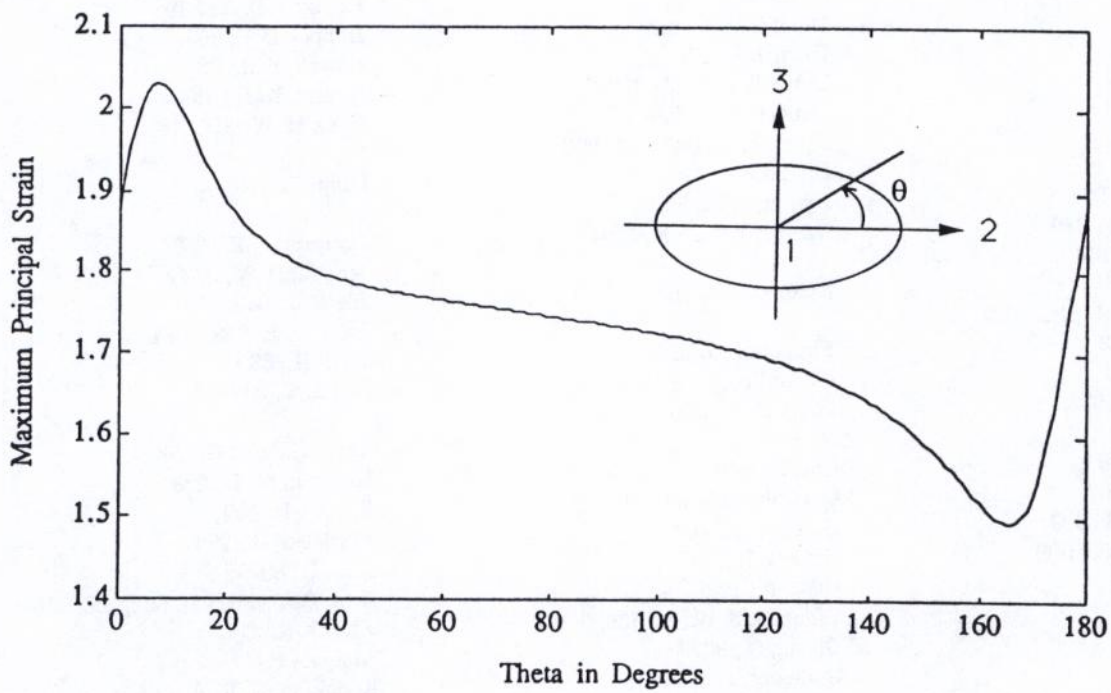


Figure 4. Distribution of Strain Concentration Factor in the Host, under Equal Bending and Actuation Loads.

Author Index

- Abrams, F., 59
Abrate, S., 125
Abuelfoutouh, N. M., 1094
Adeli, H., 1260
Advani, S. G., 103
Agarwal, R. K., 519
Albers, R. G., 587
Alghamdi, A., 919
Al-Moussawi, H. M., 876
Amateau, M. F., 228
Anand, K., 481, 493
Andersen, S. M., 565
Armstrong-Carroll, E., 1022
- Bakis, C. E., 779
Banerjee, R., 539
Bar-Cohen, Y., 410
Barron, D., 597
Baxter, W. J., 615
Benedetto, E. E., 804
Bhagat, R. B., 168, 389
Binienda, W. K., 1114
Birger, A. B., 634
Bogdanovich, A. E., 634, 1084
Breivik, N. L., 972
Brown, T. L., 1180
Bruschke, M. V., 103
- Canumalla, S., 389
Carapella, E. E., 317
Carman, G. P., 889, 909
Case, S. W., 817, 889, 909
Chang, F.-K., 1136
Chang, Y. S., 817
Chapon, E., 705
Chen, J., 339
Chen, K. L., 716
Chen, M. H., 1170
Chen, P. C. T., 1239
Chien, H. T., 757
Chinsirikul, W., 42
Choo, V. K., 757
Chou, T. W., 400, 695
Chung, T. C., 42
- Claus, S. J., 258
Clotfelter, K. L., 450
Cochran, R., 12
Coffin, D. W., 159
Conway, J. C., Jr., 389
Conway, T. A., 745
Crasto, A. S., 181, 604
Creasy, T. S., 159
- Dartford, D., 493
Dasgupta, A., 919, 1160, 1170
Datta, S. K., 380
Davis, L. C., 339
Dillard, D. A., 817
Ditri, J. J., 371
Donnellan, T. M., 1022
Doucet, A. B., 735
Drzal, L. T., 286, 837, 876
Du, S., 3
Dynan, S. A., 389
Dzenis, Y. A., 266, 1084
- Emery, A. F., 792
- Flanagan, G., 1220
Florentine, R. A., 147
Fogg, B. R., 909
- Gao, Z., 866
Garfinkle, M., 938
Gates, T. S., 207
Gavara, R., 198
Gilat, A., 1041
Gillespie, J. W., Jr., 135, 565
Gläser, G., 837
Goldberg, R. K., 349
Grady, J. E., 716
Green, D. J., 389
Greenhalgh, S., 938
Greif, R., 705
Griffin, O. H., Jr., 317, 972
Groleau, M. R., 804
Grubb, D. T., 529
Gunderson, S. L., 460
- Gupta, V., 481, 493
Gürdal, Z., 650, 972
- Haftka, R. T., 650
Hahn, H. T., 359, 779
Haq, I. U., 191
Harrison, I. R., 42
Herakovich, C. T., 1125
Hernandez, R. J., 198
Herrera-Franco, P. J., 837
Hiel, C., 1149
Holmes, S. T., 135
Hopkins, D. A., 349
Hoppel, C. P., 509
Howell, P. R., 22
Huang, K. H., 1160
Hyer, M. W., 317, 1180
- Ishai, O., 1149
- Jayaraman, K., 866
Jensen, D. W., 672
Jih, C. J., 949
Joshi, S. P., 929, 1084
Ju, T.-H., 380
Juska, T., 238
- Karandikar, P. G., 695
Karasek, M. L., 228
Karpur, P., 420
Kawiecki, G., 899
Kim, C., 80
Kim, R. Y., 181, 471, 604, 1061
Kim, Y. K., 69
Kishore, P. V., 827
Kodokian, G. K. A., 565
Koudela, J. L., 662
Krishnamurthy, S., 420
Kryaska, M., 481
- Lagace, P. A., 991
LaMattina, B., 1051
Lamontia, M. A., 565
Larson, B. K., 286